Ionic Fragmentation Mechanisms of 2,2,2-Trifluoroethanol Following Excitation with Synchrotron Radiation

Yanina B. Bava,[a] Yanina Berrueta Martínez,[a] Angélica Moreno Betancourt,[a] Mauricio F. Erben,[a] Reinaldo L. Cavasso Filho,[b] Carlos O. Della Védova,[a] and Rosana M. Romano*[a]

Gaseous 2,2,2-trifluoroethanol (TFE) is excited with synchrotron radiation between 10 and 1000 eV and the ejected electrons and positive ions are detected in coincidence. In the valence-electron energy region, the most abundant species is CH_2OH^+. Other fragments, including ions produced by atomic rearrangements, are also detected; the most abundant are COH^+, CFH_2^+ and $CF_2H_2^+$. The energies of electronic transitions from C 1s, O 1s and F 1s orbitals to vacant molecular orbitals are determined. A site-specific C 1s excitation is observed. The photofragmentation mechanisms after the excitation of core-shell electrons are inferred from analysis of the shape and slope of the coincidence between two charged fragments in the bi-dimensional coincidence spectra. The spectra are dominated by islands that correspond to the coincidence of H^+ with several charged fragments. One of the most important channels leads to the formation of CH_2OH^+ and CF_3^+ in a concerted mechanism.

1. Introduction

2,2,2-Trifluoroethanol (TFE) is a colourless liquid with a wide variety of applications, ranging from chemical reagents and polar organic solvents to biochemical and industrial uses. TFE is extensively used as a co-solvent because it promotes or stabilises the formation of the secondary structure of peptides and proteins;[1,2] this property has resulted in several studies on the structure and interactions present in the liquid phase.[3] TFE presents several industrial applications, such as pharmaceutical uses as a starting material for some inhalation anaesthetics,[4] use in the preparation and treatment of nylon,[5] and as a working fluid for heat engines.[6]

Fluorinated alcohols, and TFE in particular, are considered to be potential industrial alternative compounds for chlorofluorocarbons and hydrochlorofluorocarbons; these are the species responsible for ozone depletion in the stratosphere with high global warming potential.[7–11] In this context, the potential environmental effect of TFE was evaluated.[7,8,12] Because this molecule is photochemically stable when exposed to light available in the troposphere,[13] the main loss process in this region is the reaction with the OH⋅ radical. According to studies reported in the literature, TFE has a tropospheric lifetime of 106[12]–117[7] days, and a negligible contribution towards global warming.[7,12] TFE was also found as a product of the photolysis of 3,3,3-trifluoropropaldehyde in air, either from the self-reaction of $CF_3CH_2O_2$ radicals or through the reaction of CF_3CH_2O radicals with CF_3CH_2CHO.[14] The atmospheric surface abundance of TFE was modelled, and showed three distinctive maxima over industrialised regions of the northern hemisphere that reflected surface emissions. Variation of the concentration with altitude was also predicted.[7]

Contaminants with a relatively high tropospheric lifetime, such as TFE, can reach the ionosphere, which is the atmosphere region lying above the stratosphere dominated by photoionisation and photofragmentation processes originating from the interaction of the molecules with vacuum ultraviolet (VUV) and soft X-ray radiation. Synchrotron radiation is an ideal mimic of solar light, and hence, a very important tool for atmospheric studies.[15]

TFE exists in the gas phase as a mixture of *gauche* and *trans* conformers, as determined by vibrational spectroscopy;[16,17] the *gauche* form is the preferred conformer and is stabilised by strong H⋯F hydrogen-bond interactions. The first ionisation potential of TFE was determined by photoelectron spectroscopy at 11.74 eV.[18] Although core-electron excitation and ionisation studies of TFE in the gas phase were not previously reported, an investigation into the ionisation of C 1s electrons of a monolayer of TFE chemisorbed on a Si(100) surface was performed and site-specific fragmentation proposed.[19]

Herein, and as part of a general project aimed at elucidation of the photofragmentation mechanisms of compounds relevant for atmospheric chemistry by using synchrotron radiation, we present the study of TFE by using synchrotron radiation between 10 and 1000 eV. Valence electrons, as well as C 1s, O 1s

[a] Y. B. Bava, Y. Berrueta Martínez, Dr. A. Moreno Betancourt, Prof. Dr. M. F. Erben, Prof. Dr. Dr. C. O. Della Védova, Prof. Dr. R. M. Romano
CEQUINOR (CONICET-UNLP), Departamento de Química
Facultad de Ciencias Exactas, Universidad Nacional de La Plata
47 esq. 115, (1900) La Plata (Argentina)
romano@quimica.unlp.edu.ar

[b] Prof. Dr. R. L. Cavasso Filho
Universidade Federal do ABC, Rua Catequese, 242
CEP: 09090-400 Santo Andre SP (Brazil)

Supporting Information for this article is available on the WWW under http://dx.doi.org/10.1002/cphc.201402669.

and F 1s electrons, were excited and the positive ions formed after ionisation were detected by means of coincidence techniques.

2. Results and Discussion

2.1. Photoionisation and Photofragmentation of TFE in the Valence-Electron Energy Region

A molecular beam of TFE was exposed to synchrotron monochromatic light between 10 and 21 eV. Simultaneously, the electron and cationic fragments produced upon photoionisation, and eventually subsequent fragmentation events, were collected in coincidence. The relative intensities of the positive ions were plotted against their m/z ratio in a photoelectron photoion coincidence (PEPICO) spectrum. The pressure of the sample was maintained below 2.10^{-6} mbar during the experiments, which assured that only fragments arose from unimolecular mechanisms. The presence of more than one signal in the PEPICO spectra originated from alternative fragmentation mechanisms; thus, the relative intensity of the fragment in the spectrum indicated the relative probability of the mechanism.

Selected PEPICO spectra of TFE excited with synchrotron light in the valence-electron energy region are shown in Figure 1. Table 1 lists the relative intensities of the cationic fragments for different irradiation energies. Below 12 eV, no signals are detected in the spectra, as expected from the reported value of 11.74 eV for the first ionisation potential of the molecule.[18] The first positive ion to appear in the spectra corresponds to a fragment with m/z 31, which is coincident, in principle, with either CH_2OH^+ and/or CF^+ species. As explained later, the signal is most plausibly assigned to the former ion, although a small proportion of the latter cannot be discarded.
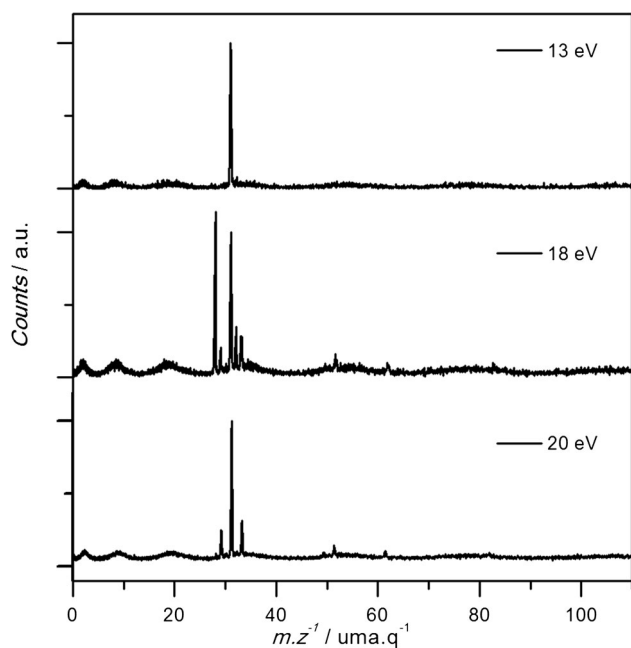
Table 1. Branching ratios [%] for positive ions extracted from PEPICO spectra as a function of the photon energies between 13 and 21 eV for TFE.

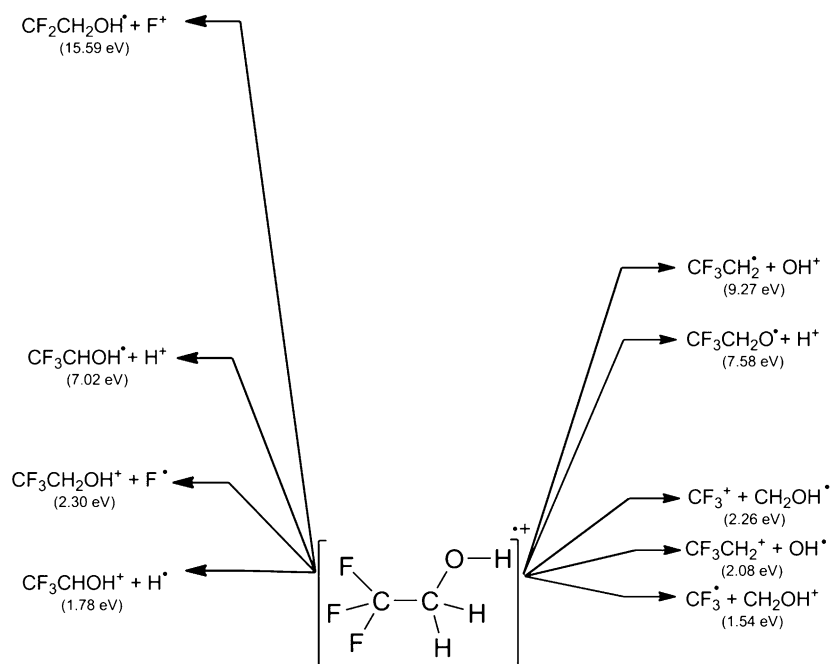| m/z | Assignment | Energy [eV] | | | | | |
		13	14	16	18	20	21
16	O^+	–	–	–	–	–	2.1
28	CO^+	–	–	3.4	79.6	1.2	11.7
29	COH^+	–	–	2.8	14.4	23.4	35.2
30	COH_2^+	–	–	2.2	3.2	1.8	3.0
31	CH_2OH^+	100.0	100.0	100.0	100.0	100.0	100.0
32	CFH^+	5.2	4.9	1.6	22.6	1.8	5.1
33	CH_2F^+	–	–	3.6	27.4	29.8	33.2
50	CF_2^+	–	–	–	1.3	2.9	2.8
52	$CF_2H_2^+$	–	–	4.0	12.5	10.0	8.9
62	$CFCH_2OH^+$	–	–	11.3	10.6	8.3	7.4
83	$CF_3CH_2^+$	–	–	5.4	3.9	6.3	5.8

The m/z 31 signal remains the most intense one in all spectra measured in this energy region; this reveals that the rupture of the C–C bond is the most important mechanism [Eq. (1)]. On the other hand, no evidence of the molecular ion is observed in the spectra, even at energies just above the first ionisation potential, which reveals the instability of $M^{+\bullet}$ and its tendency towards fragmentation.

$$CF_3-CH_2OH^{+\bullet} \rightarrow CF_3^{\bullet} + CH_2OH^+ \tag{1}$$
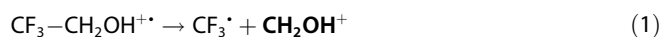
As the excitation energy increases, alternative fragmentation channels are opened, as observed in Table 1. In addition to CH_2OH^+, $CF_3CH_2^+$ is the only detected fragment originating from the rupture of only one bond. The other mechanisms involve the breaking of two ($CFCH_2OH^+$, CF_2^+, $CHOH^+$ and O^+) or three (COH^+) bonds, and also atomic rearrangements ($CF_2H_2^+$ and CH_2F^+). To better understand the fragmentation mechanisms, both the calculated relative energies of the possible fragments with respect to the molecular ion and the predicted energy and character of the HOMO orbitals were analysed.

Considering the breaking of only one of the five different bonds of $M^{+\bullet}$ (C–C, C–O, O–H, C–H or C–F), ten mechanisms are feasible, depending on which of the two fragments maintains the positive charge after rupture (see Figure 2). The energy differences between the products of these ten mechanisms and the molecular ion were calculated by using the UB3LYP/6-311+G(d,p) theoretical approximation. Each species was optimised by simultaneous relaxation of all geometrical parameters. The optimised structure of TFE$^{+\bullet}$ presents the *gauche* conformation, whereas the *anti* form does not correspond to an energy minimum for the cation. A comparison between the calculated geometrical parameters of TFE$^{+\bullet}$ and the *gauche* and *anti* forms of neutral TFE is presented in Table S2 in the Supporting Information.

The calculated energy differences for the different mechanisms are depicted in Figure 2. The energetically favoured fragments correspond to those produced by the mechanisms depicted in Equation (1), 1.54 eV above $M^{+\bullet}$, in coincidence with experimental findings. The other possibility for C–C breaking,

Figure 1. PEPICO spectra of TFE irradiated with 13, 18 and 20 eV synchrotron light.

These are not the final page numbers! ↗↗

Figure 2. Relative energies for different possible fragments of TFE$^+$ calculated with the UB3LYP/6-311+G(d) approximation.

in which CF$_3^+$ is formed, is predicted to have higher energy, which explains the lack of this ion in the spectra. CF$_3$CH$_2^+$ formation, as well as the absence of OH$^+$, is also consistent with the calculated energy differences for each mechanism that follows rupture of the C—O bond with respect to $M^{+\cdot}$ (2.08 and 9.27 eV, respectively). On the other hand, the production of H$^+$ (either from the rupture of O—H or C—H bonds) and F$^+$ (from the rupture of one of the C—F bonds) are disfavoured with respect to CF$_3$CH$_2$O$^+$, CF$_3$CHOH$^+$ and CF$_2$CH$_2$OH$^+$, respectively. However, none of these three fragments were detected in the spectra. One possible explanation would be the subsequent fragmentation of these ions, for example, CFCH$_2$OH$^+$ and CF$_2^+$, which could originate from CF$_2$CH$_2$OH$^+$; CHOH$^+$ could originate from CF$_3$CHOH$^+$; and O$^+$ could originate from CF$_3$CH$_2$O$^+$.

Variation of the ion branching ratios in the PEPICO spectra with the excitation energy presents a curious discontinuity for the spectrum recorded at 18 eV. As observed from the results given in Table 1 and Figure 1, there is a clear increase in the proportion of CO$^+$ and CFH$^+$ with respect to the ion branching ratios observed for spectra taken at other energies. To explain this unexpected behaviour, the character of the molecular orbitals (MOs) with energies close to the incident radiation, which could be selectively excited, were considered. Although the photoelectron spectrum of TFE was previously reported,[18] the energy values of the valence-electron ionisations, with the exception of the first ionisation potential, and the character of these electrons were not mentioned. A later photoelectron study of compounds containing the trifluoromethyl group reported only a correlation diagram, which showed that the orbitals of the CF$_3$ group of the TFE molecule were below 17 eV.[20] For this reason, the HOMOs of TFE were calculated by using the OVGF and P3 methods, together with the 6-311+G(d,p)

basis set, on the *gauche* molecular structure optimised at the B3LYP/6-311+G(d,p) level. The calculated vertical ionisation energies, assignment, and schematic representation of the 10 HOMOs of TFE are given in the Supporting Information. In particular, HOMO-7 and HOMO-8, with predicted vertical ionisation energies of 17.88 and 18.08 eV, are assigned to electrons formally located at the bonding σ(C—H) MOs. Thus, the selective excitation of these electrons could be the first step in the mechanisms responsible for the high yield of the CO$^+$ and CFH$^+$ fragments observed when the sample is irradiated with 18 eV light. Another fragment formed by atomic rearrangements plausibly originates from C—H ruptures to form CF$_2$H$_2^+$, which also presents a relative intensity maximum at 18 eV.

2.2. Photoionisation and Photofragmentation of TFE in the Core-Electron Energy Regions

The fragmentation mechanisms of TFE after excitation and/or ionisation of core electrons (C1s, O1s and F1s) were also studied. In the first place, the energies of resonant electron excitations, as well as the ionisation edges for each of the core electrons, were determined by detecting the positive ions produced as a function of the photon energy, without discrimination of the m/z ratio of the ions [total ion yield (TIY) spectra].

Figure 3 presents the average of three TIY spectra of TFE between 280 and 310 eV, recorded at energy intervals of 0.1 eV between 290 and 300 eV and intervals of 0.5 eV for the ranges 280–290 and 300–310 eV, with an acquisition time of 3 s at each energy step. In this energy region, electrons located at the 1s core levels of the carbon atoms are excited and/or ionised. The assignment of features observed in the TIY spectrum, as summarised in Table 2, was performed based on reports of related molecules, and are also in accordance with predictions obtained by theoretical calculations (see below).

Selective core-electron excitation and ionisation is observed for each of the carbon atoms of the molecule. The ionisation threshold of the 1s electrons of the methylene carbon atom, C$_{(H)}$ 1s, is observed at 291.5 eV, whereas that corresponding to the trifluoromethyl carbon, C$_{(F)}$ 1s, occurs at 298.0 eV.[21] The 6.5 eV energy difference exactly coincides with the energy observed for CF$_3$CH$_3$,[19,22] and with the general behaviour of different fluorinated saturated and unsaturated organic molecules, for which a chemical shift of about 2.2 eV per fluorine atom was determined.[19,23,24] Below the C$_{(H)}$ 1s threshold, three
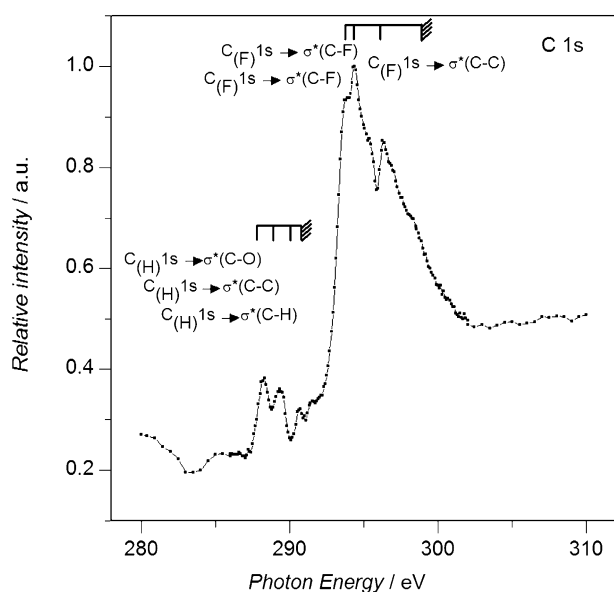
These are not the final page numbers! ↗↗

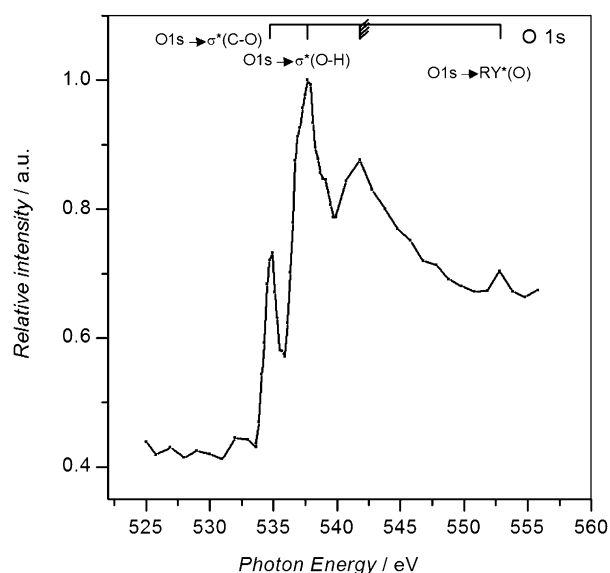**Figure 3.** Total ion yield (TIY) spectrum of TFE in the C 1s energy region.

Figure 4. TIY spectrum of TFE in the O 1s energy region.

Table 2. Energies [eV] and proposed assignment of the features observed in the TIY spectra of TFE excited in the C 1s, O 1s and F 1s regions.	
Energy [eV]	Assignment[a]
288.2	$C_{(H)}$ 1s→σ*(C–O)
289.3	$C_{(H)}$ 1s→σ*(C–C)
290.7	$C_{(H)}$ 1s→σ*(C–H)
291.5	IP $C_{(H)}$ 1s
293.9	$C_{(F)}$ 1s→σ*(C–F)
294.5	$C_{(F)}$ 1s→σ*(C–F)
296.5	$C_{(F)}$ 1s→σ*(C–C)
298.0	IP $C_{(F)}$ 1s
534.9	O 1s→σ*(C–O)
537.7	O 1s→σ*(O–H)
541.8	IP O 1s
552.8	O 1s→Rydberg
692.0	F 1s→σ*(C–F)
694.2	F 1s→σ*(C–C)
695.2	IP F 1s
[a] IP = ionisation potential.	

The TIY spectrum of TFE around the O 1s energy is depicted in Figure 4. Three spectra were averaged, recorded with an energy interval of 0.2 eV between 533 and 540 eV and an interval of 1.0 eV for the ranges 525–533 and 540–555 eV, with an acquisition time of 2 s at each energy interval. The spectrum presents two strong resonances, localised at 534.9 and 537.7 eV, which are assigned to O 1s→σ*(C–O) and O 1s→σ*(O–H) transitions, and the ionisation threshold is observed at 541.8 eV (see Table 2). A low intensity signal at 552.8 eV was associated with the O 1s→Rydberg transition.

Figure 5 presents the TIY spectrum in the F 1s energy region. The average of three spectra measured with an energy interval of 0.2 eV between 687 and 700 eV and an interval of 1.0 eV for the ranges 670–687 and 700–720 eV, at an acquisition time of 2 s at each energy interval, was plotted. The spec-
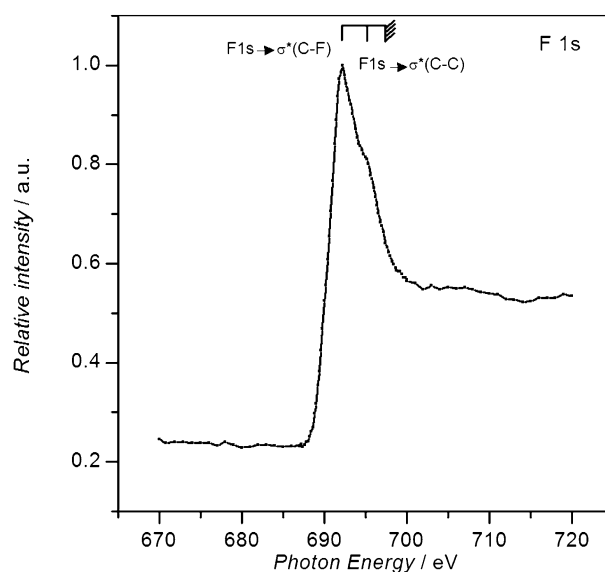
resonances were detected at 288.2, 289.3 and 290.7 eV, which were assigned to $C_{(H)}$ 1s→σ*(C–O), $C_{(H)}$ 1s→σ*(C–C) and $C_{(H)}$ 1s→σ*(C–H) transitions, respectively. The most intense bands of the spectra, at 293.9, 294.5 and 296.5 eV, were associated with transitions of $C_{(F)}$ 1s→σ*(C–F) and $C_{(F)}$ 1s→σ*(C–C). The intensification of $C_{(F)}$ 1s→σ* transitions in C 1s spectra upon fluorination was previously reported; in some cases, with even greater oscillator strength than $C_{(F)}$ 1s→π*.[24]

The C 1s site-specific excitation is also in agreement with the two broad features observed in the photoelectron spectra of a monolayer of TFE chemisorbed on a Si(100) surface, which was assigned to $C_{(H)}$ 1s→σ* and $C_{(F)}$ 1s→σ*.[19] Although the energy of these transitions was not reported, approximate values of 290.5 and 297.0 eV for the transitions originating from the $C_{(H)}$ 1s and $C_{(F)}$ 1s orbitals, respectively, could be inferred from the total electron yield spectrum; this is in complete accordance with our results.

Figure 5. TIY spectrum of TFE in the F 1s energy region.

trum presents a strong resonance at 692.0 eV, which is assigned to F 1s→σ*(C–F) transitions, and an unresolved feature at approximately 694.2 eV associated with a F 1s→σ*(C–C) transition. The F 1s ionisation threshold is observed at 695.2 eV.

The relative energies and approximately character of the LUMOs were calculated for the *gauche* and *anti* conformers of TFE at the B3LYP/6-311+G** level of approximation. No significant differences were found for either conformer. The three lowest LUMOs, LUMO, LUMO+1 and LUMO+2, correspond to σ*(C–F) orbitals. Small differences of 0.01–0.02 eV, which are out of range of experimental resolution of the TIY spectra, are predicted for these MOs. This prediction is in accordance with lowering of the σ*(X–F) orbitals reported for molecules containing fluorine atoms, and is known as the weak-bond effect.[24,25] LUMO+3 and LUMO+4 present σ*(C–O) and σ*(C–C) character; the two next MOs correspond to σ*(C–H) with energy differences of about 0.01 eV, as predicted for the σ*(C–F) orbitals; and LUMO+7 corresponds to σ*(O–H) MO.

The data extracted from the TIY spectra of TFE (Table 2) can be combined to construct an experimental MO picture. The observed transitions are illustrated in Figure 6, and the energy
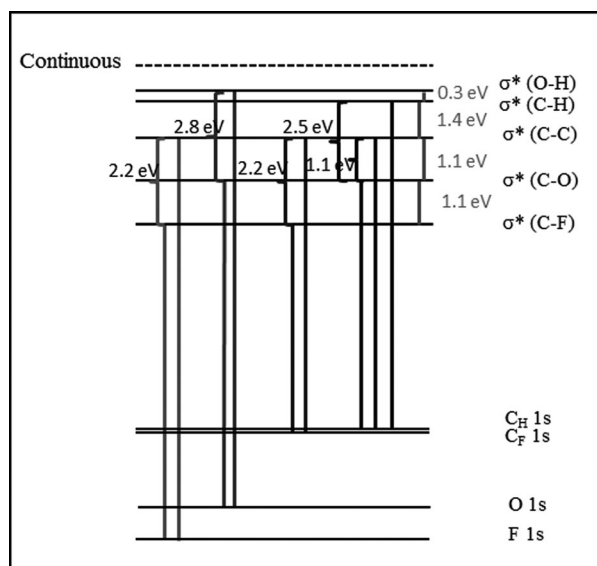

Figure 6. MO scheme constructed with data extracted from the TIY spectra of TFE.

differences between the LUMOs calculated from these data. The order of the antibonding sigma orbital deduced from the experimental values coincides with the prediction of the theoretical calculations described above.

The core hole states originating from excitation or ionisation of 1s electrons can relax by emission of Auger electrons and subsequent formation of a doubly charged ion. This highly charged ion usually results in two singly charged fragments and eventually also in neutral species. The PEPICO spectra present only the lightest ion in coincidence with the ejected electron (again, the low sample pressure maintained in the ex-

perimental chamber guarantees only signals arising from unimolecular processes).

PEPICO spectra of TFE were measured at resonant and threshold excitation energies of C 1s, O 1s and F 1s electrons, as described above. Figure 7 shows the spectrum measured at
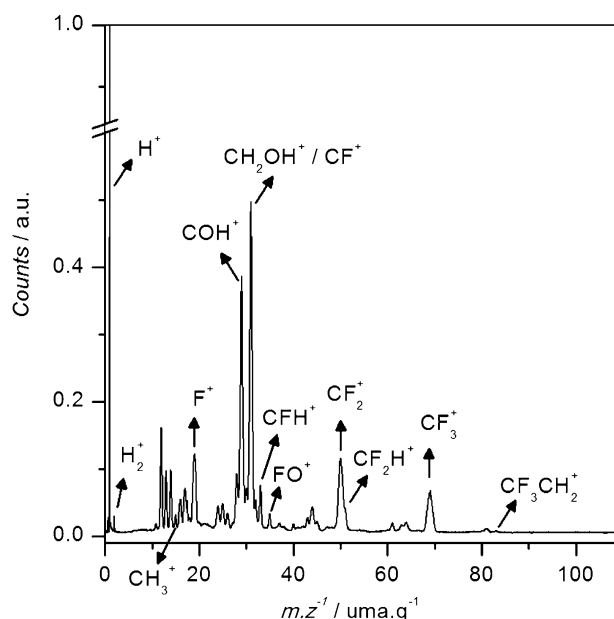
Figure 7. PEPICO spectrum of TFE measured at 294.5 eV.

294.5 eV, together with the assignment of the most abundant peaks. Spectra taken at different energies and a complete list of the fragments, their assignment and relative abundances are presented in Table 3 and Figure S1 in the Supporting Information.

All fragments with $m/z > 50$ ($M^{+\bullet} = 100$) must arise from a single ionisation process. The most intense of this group of signals corresponds to CF_3^+ (m/z 69), as observed in Figure 7. The mechanism described by Equation (2), which was not detected for excitation in the valence region, was then opened at core-electron photon energies.

$$CF_3-CH_2OH^{+\bullet} \rightarrow \mathbf{CF_3^+} + CH_2OH^\bullet \qquad (2)$$
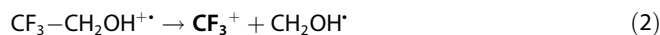
The relative abundance of CF_3^+ clearly varies with the excitation energies and reaches a maximum of approximately 14% for the $C_{(F)}$ 1s→σ*(C–C) resonance and a minimum ($\approx$1%) when the $C_{(H)}$ 1s electrons are selectively excited. Other ions due to single ionisations detected are as follows: $CF_2CH_2OH^+$; $CF_xH_y^+$, with $(x,y) = (3,2)$, $(2,2)$ and $(2,1)$; $CFCH_2O^+$; and CF_2H^+. The last fragment, which originates from only an atomic rearrangement, presents an enhancement of approximately four times that of the $C_{(F)}$ 1s→σ*(C–C) resonance, and completely disappears for the F 1s excitation.

The signal at m/z 50 can be assigned to either CF_2^+ or FCH_2OH^+ ions (strictly speaking, the signal can also be attributed to TFE^{2+}, but this seems very improbable upon considering the 8–9% observed abundance of this fragment). The lack of

Table 3. Branching ratios [%] for fragment ions extracted from PEPICO spectra of TFE as a function of the photon energies in the C 1s, O 1s and F 1s energy regions.

m/z	Assignment	Energy [eV]						
		288.2	294.5	296.5	534.9	537.7	692.0	707.0
1	H^+	5.0	5.2	4.6	6.9	6.4	5.4	5.9
2	H_2^+	0.2	0.2	0.2	0.4	0.2	0.2	0.2
3	H_3^+	<0.1	<0.1	<0.1	<0.1	<0.1	<0.1	<0.1
12	C^+	1.7	4.7	4.2	6.0	5.6	6.6	6.4
13	CH^+	1.2	2.7	2.	2.8	3.1	3.2	2.9
14	CH_2^+	27.4	2.6	2.2	2.6	3.0	2.6	3.4
15	CH_3^+	0.0	0.3	0.2	0.4	0.3	0.2	0.2
16	O^+	23.1	2.6	0.2	4.6	5.6	3.1	4.0
17	OH^+	1.8	3.4	2.2	2.5	3.3	3.8	4.0
18	H_2O^+	0.7	0.7	0.2	0.0	0.1	0.8	0.0
19	F^+	3.9	8.0	6.2	9.1	9.0	12.4	10.2
20	HF^+	2.8	0.4	0.6	0.0	0.0	0.0	0.0
24	C_2^+	0.4	2.0	1.6	1.3	2.2	2.0	1.9
25	C_2H^+	0.6	1.9	1.6	0.4	1.7	2.0	1.1
26	$C_2H_2^+$	0.3	0.7	0.5	0.6	0.8	0.9	0.4
27	$C_2H_3^+$	0.0	0.0	0.6	0.0	0.0	0.0	0.0
28	CO^+	4.1	3.5	3.1	1.9	2.0	4.0	2.6
29	COH^+	7.4	15.4	13.5	11.7	11.0	14.7	15.4
30	CH_2O^+	1.4	<0.1	0.5	0.3	0.2	0.2	0.2
31	CH_2OH^+/ CF^+	9.3	18.1	15.9	17.3	15.5	18.8	19.3
32	CFH^+	1.8	1.5	1.4	2.8	2.2	0.9	1.4
33	CH_2F^+	0.9	1.4	0.9	1.2	1.3	0.6	0.8
35	FO^+	0.0	0.6	0.5	1.5	0.2	0.1	0.2
38	F_2^+	0.0	<0.1	0.1	0.0	0.1	0.1	0.2
40	C_2O^+	0.0	0.3	0.6	0.4	0.3	0.3	0.3
43	$C_2H_2OH^+$	0.0	0.7	0.8	0.2	1.1	0.9	1.1
44	C_2FH^+	0.4	1.7	2.4	0.9	2.6	1.6	1.2
45	$C_2FH_2^+$	0.0	0.3	0.2	1.0	0.7	0.4	0.5
50	CF_2^+/ FCH_2OH^+	3.2	9.8	8.2	8.9	9.0	7.5	8.6
51	CF_2H^+	0.0	1.1	4.5	1.9	1.2	0.0	0.0
61	$C_2FOH_2^+$	0.3	0.4	0.5	0.3	0.2	0.1	0.1
63	$C_2F_2H^+$	0.0	0.5	0.9	0.4	0.8	0.4	0.6
64	$C_2F_2H_2^+$	0.2	0.3	0.5	1.0	0.7	0.4	0.4
69	CF_3^+	1.2	7.8	13.8	8.02	8.4	4.1	5.3
81	$CF_2CH_2OH^+$	0.0	0.4	0.7	0.00	0.1	0.2	0.2
83	$CF_3CH_2^+$	0.0	0.1	0.2	0.24	0.3	<0.1	0.2

From the complete list of relative branching ratios presented in Table 3, moderate site-specific fragmentation can be assumed.

The photoelectron photoion photoion coincidence (PEPIPICO) technique detects the lightest ion (in the T_1 domain) and the second lightest ion (in the T_2 domain) produced by unimolecular photofragmentation as a consequence of a double photoionisation process in coincidence with ejected electrons. The shape and slope of the coincidence islands of the PEPIPICO spectra contain valuable information about the fragmentation dynamics.

Bi-dimensional PEPIPICO spectra of TFE were measured at each resonance and ionisation thresholds of the C 1s, O 1s and F 1s edges. The shape and slope of the most intense coincidences were almost independent of the incident radiation, which indicated that the dynamic of the fragmentations, but not their probability, were not site specific. The spectra are dominated by islands that correspond to the coincidence of H^+ with several charged fragments. Figure 8 shows the T_1 and T_2 projections of the PEPIPICO spectra of TFE recorded at 294.5 eV.

Figure 8. T_1 and T_2 projections of the PEPIPICO spectrum of TFE recorded at 294.5 eV
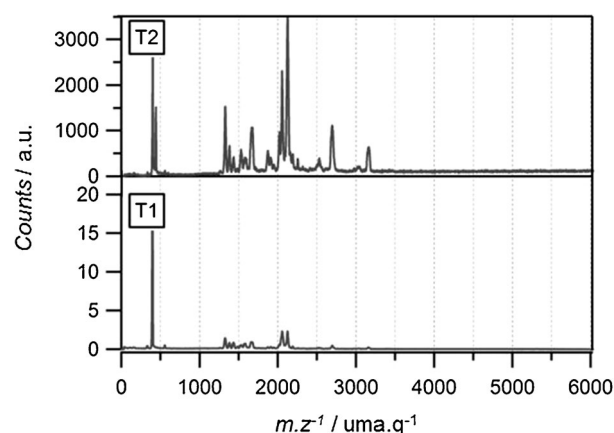
a coincidence of two ions with m/z 50 in the PEPIPICO spectra, as discussed below, confirms that this fragment comes from a singly charged molecular ion. However, there is no experimental evidence to decide which fragment (CF_2^+, FCH_2OH^+ or both) contributes to the m/z 50 signal.

Several signals are observed in the PEPICO spectra with m/z <50: $C_2H_nF^+$, $n = 0–2$; $C_2H_2OH^+$; F_2^+; FO^+; CH_nF^+, $n = 0–2$; CH_nO^+, $n = 0–3$; $C_2H_n^+$, $n = 0–3$; HF^+; F^+; OH_n^+, $n = 0–2$; CH_n^+, $n = 0–3$; and H_n^+, $n = 1–3$. CH_2OH^+ and COH^+ are the most intense ions, with abundances higher than 15 and 11 %, respectively, at all studied energies, except when the sample is irradiated at the $C_{(H)}$ 1s resonances, for which the most intense fragments of the spectra are CH_2^+ (27 %) and O^+ (23 %). The production of CH_3^+, HF^+, CHF^+, CH_2F^+, FO^+ and F_2^+ ions can only be explained by atomic rearrangement. FO^+ is selectively formed in the O 1s→σ*(C–O) resonance ($\approx$1.5 %) and the formation of F_2^+ is favoured after F 1s ionisation. In addition to H_2^+, very weak features of H_3^+ are observed in the spectra.

The photofragmentation mechanisms of TFE were inferred from analysis of the shapes and slopes of the coincidences between two charged fragments in the bi-dimensional PEPIPICO spectra, following the formalisms proposed by Eland.[26] In these formalisms, the requirement for conservation of the linear momentum of the fragments allows the deduction of the theoretical slope of the coincidence islands, according to different proposed mechanisms. Inspection of the spectra reveals that the fragmentation channels involve the rupture of more than one chemical bond, with the exception of the mechanism in Equation (3):

$$CF_3-CH_2OH^{2+} \rightarrow CF_3^+ + CH_2OH^+ \tag{3}$$

These are not the final page numbers! ↗↗

As in case of the mechanisms described by Equations (1) and (2) for the fragmentation of the singly charged molecular ion, this channel originates from C–C bond breaking in a concerted dissociation (CD) channel. The parallelogram shape and experimental slope, $\alpha_{exptl} = 1.00$, of the CH_2OH^+/CF_3^+ island coincides with the expected slope for this two-body concerted mechanism.

Figures 9 and 10 depict the contour maps of the COH^+/CF_3^+ and COH^+/CF_2^+ islands, respectively. Both coincidences present a parallelogram shape and $\alpha_{exptl} = 1.06$, which can be explained by secondary decay (SD; $\alpha_{calcd} = 1.06$) and secondary decay after deferred charged separation (SD-DCS; $\alpha_{calcd} = 1.06$) mechanisms, respectively [Eqs. (4) and (5)].
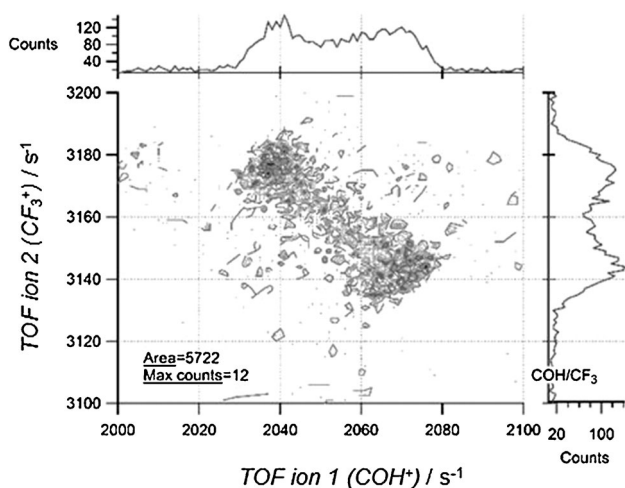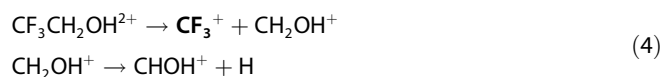
$$CF_3CH_2OH^{2+} \rightarrow \mathbf{CF_3^+} + CH_2OH^+$$
$$CH_2OH^+ \rightarrow CHOH^+ + H \quad\quad (4)$$

$$CHOH^+ \rightarrow \mathbf{COH^+} + H$$
$$CF_3CH_2OH^{2+} \rightarrow CF_2CH_2OH^{2+} + F$$
$$CF_2CH_2OH^{2+} \rightarrow \mathbf{CF_2^+} + CH_2OH^+ \quad\quad (5)$$
$$CH_2OH^+ \rightarrow CHOH^+ + H$$
$$CHOH^+ \rightarrow \mathbf{COH^+} + H$$

The signal at m/z 31 can correspond, in principle, to either CH_2OH^+ or CF^+ fragments. The bi-dimensional PEPIPICO spectra show that both ions are produced because the CH_2OH^+/CF^+, CH_2OH^+/CF_2^+ and H^+/CF^+ coincidences are observed.

The most abundant islands of the PEPIPICO spectra involve a H^+ fragment, which arrives in coincidence with H^+, H_2^+, CH_x^+ ($x = 0, 1, 2$), O^+, OH^+, F^+, COH^+, CF^+, CF_2^+ and CF_3^+ (Figure 11). All of these islands present an ovoid shape, as depicted, for example, for the H^+/CF^+ coincidence in Figure 12; this indicates a concerted mechanism [Eq. (6)].

$$CF_3CH_2OH^{2+} \rightarrow \mathbf{CF^+} + \mathbf{H^+} + \text{neutral fragments} \quad\quad (6)$$

Figure 9. Contour map of the COH^+/CF_3^+ coincidence island in the PEPIPICO spectrum of TFE recorded at 294.5 eV.

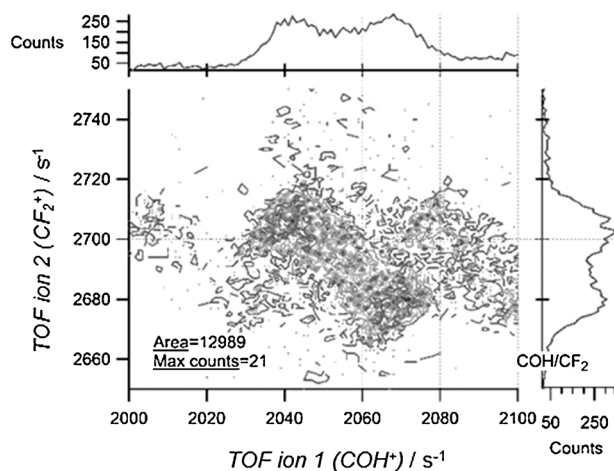**Figure 11.** T_2 projections of the PEPIPICO spectrum of TFE in coincidence with H^+ in T1, recorded at 294.5 eV.

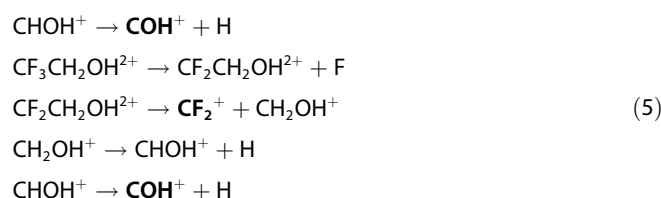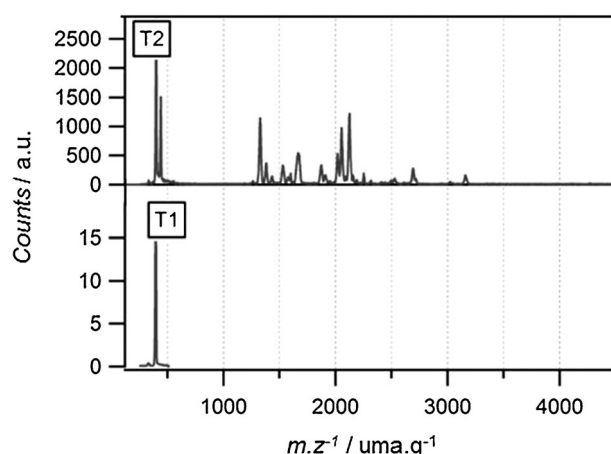**Figure 10.** Contour map of the COH^+/CF_2^+ coincidence island in the PEPIPICO spectrum of TFE recorded at 294.5 eV.

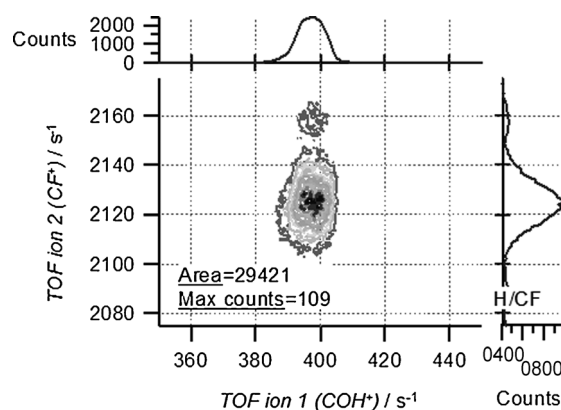**Figure 12.** Contour map of the H^+/CF^+ coincidence island in the PEPIPICO spectrum of TFE recorded at 294.5 eV.

These are not the final page numbers! ↗↗

The shape of the island H^+/H_2^+ is also coincident with concerted mechanisms, which additionally involve an atomic rearrangement. All fragmentation channels of TFE^{2+} that form a proton also result in breaking of the C—C bond.

3. Conclusions

The photoexcitation, photoionisation and photofragmentation mechanisms of gaseous TFE were studied by using synchrotron radiation in the valence electron and C, O, and F K-shell energy regions by using coincidence techniques. Irradiation of the sample with a photon energy just above the first ionisation potential resulted in rupture of the C—C bond and formation of the CH_2OH^+ fragment; this was in agreement with the energetically favoured mechanism, according to density functional theory calculations. Although alternative channels are opened at higher energies, CH_2OH^+ remains the most important fragment. A discontinuity is observed for the excitation with 18 eV, with a strong enhancement of CO^+ and, to a lesser extent, of CFH^+. These preferred mechanisms at a particular energy were proposed to arise from the resonance of the excitation energy with the ionisation of electrons located at the σ(C—H) MOs.

The energies of the excitations of K-shell electrons to vacant MOs, as well as their ionisation edges, were determined by TIY spectra. Selective excitation and ionisation of the 1s electron of each of the carbon atoms of the molecules was observed. In accordance with previous reports,[23] a 6.5 eV energy difference for $C_{(F)}$ 1s and $C_{(H)}$ 1s, about 2.2 eV per F atom, was determined. By combining the resonances from the three core shells to the vacant orbitals, a scheme with the relative energy order of the LUMOs could be proposed.

Several different fragmentation mechanisms after core excitation of TFE were detected. Although moderate site-specific fragmentation was observed, the dynamics of the mechanisms were independent of the incident radiation. The most probable channels involved a proton and another positive fragment, which originated from concerted mechanisms. The behaviour of TFE differed from that of its analogue ethanol,[27] since the molecular ion is observed in the latter even after core-electron excitation.

Although H_3^+ was detected in fragmentation studies after core ionisation in other alcohols, for example, $CH_3OH^{[28]}$ and $CH_3CH_2OH,^{[27]}$ it was attributed to the rearrangement of H atoms of the CH_3 unit. In TFE, the formation H_3^+ must involve the H atoms of the CH_2 and OH groups.

Experimental Section

The purity of a commercial sample of TFE was confirmed by means of its vapour-phase IR spectrum. The synchrotron radiation was used at the Laboratório Nacional de Luz Síncrotron (LNLS), Campinas, Sao Paulo, Brazil, in three campaigns.[29] Linearly polarised light monochromatised by a toroidal grating monochromator (TGM beamline, from 10 to 310 eV) or a by a spherical grating monochromator (available at the SGM beam line in the range 250–1000 eV)[30] intersected the effusive gaseous sample inside a high-vacuum experimental station[31] at a base pressure in the range of 10^{-8} mbar. During the experiments, the pressure was maintained below 2×10^{-6} mbar. The resolution was $\Delta E/E < 200$. The intensity of the emergent beam was recorded by a light-sensitive diode. High-purity VUV photons were used; the problem of contamination by high-order harmonics could be suppressed by the gas-phase harmonic filter recently installed at the TGM beam line at the LNLS.[32–34] The ions produced by the interaction of the gaseous sample with the light beam were detected by means of a time-of-flight (TOF) mass spectrometer of the Wiley–McLaren type for both PEPICO and PEPIPICO measurements.[35, 36] This instrument was constructed at the Institute of Physics, Brasilia University, Brasilia, Brazil.[37] The axis of the TOF spectrometer was perpendicular to the photon beam and parallel to the plane of the storage ring. Electrons were accelerated to a multichannel plate (MCP) and recorded without energy analysis. This event started the flight time determination process for the corresponding ion, which was consequently accelerated to another MCP for both PEPICO and PEPIPICO. MO calculations were performed by using the Gaussian 03 program package,[38] with the OVGF[39] and P3[40] methods, together with the 6-311+G(d,p) basis set.

Keywords: gas-phase reactions · ionization potentials · photochemistry · radicals · valence isomerization

[1] Y. Yamada, Y. Noboru, T. Sakaguchi, Y. Nibu, *J. Phys. Chem. A* **2012**, *116*, 2845–2854.
[2] B. V. Plapp, S. Ramaswamy, *Biochemistry* **2012**, *51*, 4035–4048.
[3] I. Bakó, T. Radnai, M. C. Bellisent Funel, *J. Chem. Phys.* **2004**, *121*, 12472–12480.
[4] M. D. Krasowski, N. L. Harrison, *Br. J. Pharmacol.* **2000**, *129*, 731–743.
[5] L. Francis, F. Giunco, A. Balakirshnan, E. Marsano, *Curr. Appl. Phys.* **2010**, *10*, 1005–1008.
[6] K. K. Srinivasan, P. J. Mago, S. R. Krishnan, *Energy* **2010**, *35*, 2387–2399.
[7] S. R. Sellevåg, C. J. Nielsen, O. A. Søvde, G. Myhre, J. K. Sundet, F. Stordal, I. S. A. Isaksen, *Atmos. Environ.* **2004**, *38*, 6725–6735.
[8] M. D. Hurley, T. J. Wallington, M. P. Sulbaek Andersen, D. A. Ellis, J. W. Martin, S. A. Mabury, *J. Phys. Chem. A* **2004**, *108*, 1973–1979.
[9] M. Antiñolo, S. González, B. Ballesteros, J. Albaladejo, E. Jiménez, *J. Phys. Chem. A* **2012**, *116*, 6041–6050.
[10] L. Chen, N. Takenaka, H. Bandow, Y. Maeda, *Atmos. Environ.* **2003**, *37*, 4817–4822.
[11] E. S. Vasil'ev, I. I. Morozov, W. Hack, K.-H. Hoyermann, M. Hold, *Kinet. Catal.* **2006**, *47*, 834–845.
[12] S. Dhanya, K. K. Pushpa, P. D. Naik, *Curr. Sci.* **2012**, *102*, 452–459.
[13] D. R. Salahub, C. Sandorfy, *Chem. Phys. Lett.* **1971**, *8*, 71–74.
[14] M. Antiñolo, C. Bettinelli, C. D. Jain, P. Dréan, B. Lemoine, J. Albaladejo, E. Jiménez, C. Fittschen, *J. Phys. Chem. A* **2013**, *117*, 10661–10670.

These are not the final page numbers! ↗↗

[15] N. J. Mason, A. Dawes, R. Mukerji, E. A. Drage, E. Vasekova, S. M. Webb, P. Limão-Vieira, *J. Phys. B* **2005**, *38*, S893–S911.

[16] A. J. Barnes, H. E. Hallam, D. Jones, *Proc. R. Soc. London Ser. A* **1973**, *335*, 97–111.

[17] M. Perttilä, *Spectrochim. Acta* **1979**, *35*, 585–592.

[18] M. B. Robin, N. A. Kuebler, *J. Electron Spectrosc. Relat. Phenom.* **1972**, *73*, 13–28.

[19] S. Nagaoka, S. Tanaka, K. Mase, *J. Phys. Chem. B* **2001**, *105*, 1554–1561.

[20] T. Cvitaš, I. Novak, L. Klasinc, *Int. J. Quantum Chem. Symp.* **1987**, 737–742.

[21] M. Abu-samha, K. J. Børve, L. J. Sæthre, T. D. Thomas, *Phys. Rev. Lett.* **2005**, *95*, 103002–103005.

[22] K. Müller-Dethlefs, M. Sander, L. A. Chewter, E. W. Schlag, *J. Phys. Chem.* **1984**, *88*, 6098–6100.

[23] W. Habenicht, H. Baiter, K. Müller-Dethlefs, E. W. Schlag, *J. Phys. Chem.* **1991**, *95*, 6774–6780.

[24] M. B. Robin, I. Ishii, R. McLaren, A. P. Hitchcock, *J. Electron Spectrosc. Relat. Phenom.* **1988**, *47*, 53–92.

[25] I. Ishii, R. McLaren, A. P. Hitchcock, M. B. Robin, *J. Chem. Phys.* **1987**, *87*, 4344.

[26] J. H. D. Eland, *Mol. Phys.* **1987**, *61*, 725–745.

[27] S. Pilling, H. M. Boechat-Roberty, A. C. F. Santos, G. G. B. de Souza, *J. Electron Spectrosc. Relat. Phenom.* **2007**, *1–3*, 70–76.

[28] A. Hempelmann, M. N. Piancastelli, F. Heiser, O. Gessner, A. Rüdel, U. Becker, *J. Phys. B* **1999**, *32*, 2677–2689.

[29] A. C. Lira, A. R. D. Rodrigues, A. Rosa, C. E. T. Goncalves da Silva, C. Pardine, C. Scorzato, D. Wisnivesky, F. Rafael, G. S. Franco, G. Tosin, L. Lin Jahnel, M. J. Ferreira, P. F. Tavares, R. H. A. Farias, R. T. Neuenschwander, *EPAC-98, Euro. Part. Accel. Conf. 6th* **1998**, 626.

[30] P. T. Fonseca, E. d'A Samogin, *Rev. Sci. Instrum.* **1992**, *63*, 1256–1259.

[31] F. Burmeister, L. H. Coutinho, R. R. T. Marinho, M. G. P. Homem, M. A. A. de Morais, A. Mocellin, O. Björnholm, S. L. Sorensen, P. T. Fonseca, A. Lindgren, A. Naves de Brito, *J. Electron Spectrosc. Relat. Phenom.* **2010**, *180*, 6–13.

[32] R. L. Cavasso Filho, M. G. P. Homem, R. Landers, A. Naves de Brito, *J. Electron Spectrosc. Relat. Phenom.* **2005**, *144–147*, 1125–1127.

[33] R. L. Cavasso Filho, A. F. Lago, M. G. P. Homem, S. Pilling, A. Naves de Brito, *J. Electron Spectrosc. Relat. Phenom.* **2007**, *156–158*, 168–171.

[34] R. L. Cavasso Filho, M. G. P. Homem, P. T. Fonseca, A. Naves de Brito, *Rev. Sci. Instrum.* **2007**, *78*, 115104.

[35] L. J. Frasinski, M. Stankiewicz, K. J. Randall, P. A. Hatherly, K. J. Codling, *Phys. B* **1986**, *19*, L819.

[36] J. H. D. Eland, F. S. Wort, R. N. J. Royds, *J. Electron Spectrosc. Relat. Phenom.* **1986**, *41*, 297–309.

[37] A. Naves de Brito, R. Feifel, A. Mocellin, A. B. Machado, S. Sundin, I. Hjelte, S. L. Sorensen, O. Bjorneholm, *Chem. Phys. Lett.* **1999**, *309*, 377–385.

[38] Gaussian 03, Revision B.01, M. J. Frisch, G. W. Trucks, H. B. Schlegel, G. E. Scuseria, M. A. Robb, J. R. Cheeseman, J. A. Montgomery, Jr., T. Vreven, K. N. Kudin, J. C. Burant, J. M. Millam, S. S. Iyengar, J. Tomasi, V. Barone, B. Mennucci, M. Cossi, G. Scalmani, N. Rega, G. A. Petersson, H. Nakatsuji, M. Hada, M. Ehara, K. Toyota, R. Fukuda, J. Hasegawa, M. Ishida, T. Nakajima, Y. Honda, O. Kitao, H. Nakai, M. Klene, X. Li, J. E. Knox, H. P. Hratchian, J. B. Cross, C. Adamo, J. Jaramillo, R. Gomperts, R. E. Stratmann, O. Yazyev, A. J. Austin, R. Cammi, C. Pomelli, J. W. Ochterski, P. Y. Ayala, K. Morokuma, G. A. Voth, P. Salvador, J. J. Dannenberg, V. G. Zakrzewski, S. Dapprich, A. D. Daniels, M. C. Strain, O. Farkas, D. K. Malick, A. D. Rabuck, K. Raghavachari, J. B. Foresman, J. V. Ortiz, Q. Cui, A. G. Baboul, S. Clifford, J. Cioslowski, B. B. Stefanov, G. Liu, A. Liashenko, P. Piskorz, I. Komaromi, R. L. Martin, D. J. Fox, T. Keith, M. A. Al-Laham, C. Y. Peng, A. Nanayakkara, M. Challacombe, P. M. W. Gill, B. Johnson, W. Chen, M. W. Wong, C. Gonzalez, J. A. Pople, Gaussian, Inc., Pittsburgh, PA, **2003**.

[39] L. S. Cederbaum, W. Domcke, *Adv. Chem. Phys.* **1977**, *36*, 205–344.

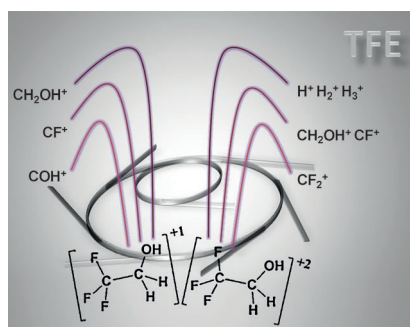[40] J. V. Ortiz, *J. Chem. Phys.* **1996**, *104*, 7599–7605.

These are not the final page numbers! ↗↗

ARTICLES

Y. B. Bava, Y. Berrueta Martínez,
A. Moreno Betancourt, M. F. Erben,
R. L. Cavasso Filho, C. O. Della Védova,
R. M. Romano*

■■ – ■■

🖳 **Ionic Fragmentation Mechanisms of 2,2,2-Trifluoroethanol Following Excitation with Synchrotron Radiation**

Breaking it down: The most important photofragmentation channel of gaseous 2,2,2-trifluoroethanol (TFE) after photoionization in the valence-electron energy region results in CH_2OH^+ and $CF_3^{\bullet}$ (see figure). After core-shell electron excitations, several fragmentation mechanisms involving two positive ions are observed; the most abundant of which produce H^+.

These are not the final page numbers! ↗↗